

REPORT DOCUMENTATION PAGE

Form Approved
OMB No. 0704-0188

Public reporting burden for this collection of information is estimated to average 1 hour per response, including the time for reviewing instructions, searching existing data sources, gathering and maintaining the data needed, and completing and reviewing this collection of information. Send comments regarding this burden estimate or any other aspect of this collection of information, including suggestions for reducing this burden to Department of Defense, Washington Headquarters Services, Directorate for Information Operations and Reports (0704-0188), 1215 Jefferson Davis Highway, Suite 1204, Arlington, VA 22202-4302. Respondents should be aware that notwithstanding any other provision of law, no person shall be subject to any penalty for failing to comply with a collection of information if it does not display a currently valid OMB control number. PLEASE DO NOT RETURN YOUR FORM TO THE ABOVE ADDRESS.

1. REPORT DATE (DD-MM-YYYY)		2. REPORT TYPE Technical Papers		3. DATES COVERED (From - To)
4. TITLE AND SUBTITLE				5a. CONTRACT NUMBER
				5b. GRANT NUMBER
				5c. PROGRAM ELEMENT NUMBER
6. AUTHOR(S)				5d. PROJECT NUMBER 2302
				5e. TASK NUMBER MLG2
				5f. WORK UNIT NUMBER 346120
7. PERFORMING ORGANIZATION NAME(S) AND ADDRESS(ES)				8. PERFORMING ORGANIZATION REPORT
Air Force Research Laboratory (AFMC) AFRL/PRS 5 Pollux Drive Edwards AFB CA 93524-7048				
9. SPONSORING / MONITORING AGENCY NAME(S) AND ADDRESS(ES)				10. SPONSOR/MONITOR'S ACRONYM(S)
Air Force Research Laboratory (AFMC) AFRL/PRS 5 Pollux Drive Edwards AFB CA 93524-7048				11. SPONSOR/MONITOR'S NUMBER(S) <i>Please see attached</i>
12. DISTRIBUTION / AVAILABILITY STATEMENT				
Approved for public release; distribution unlimited.				
13. SUPPLEMENTARY NOTES				
14. ABSTRACT				
20030205 139				
15. SUBJECT TERMS				
16. SECURITY CLASSIFICATION OF:			17. LIMITATION OF ABSTRACT	18. NUMBER OF PAGES
			A	19a. NAME OF RESPONSIBLE PERSON Leilani Richardson
a. REPORT Unclassified	b. ABSTRACT Unclassified	c. THIS PAGE Unclassified		
			19b. TELEPHONE NUMBER (include area code) (661) 275-5015	

MEMORANDUM FOR PRS (In-House Publication)

FROM: PROI (STINFO)

25 February 2002

SUBJECT: Authorization for Release of Technical Information, Control Number: **AFRL-PR-ED-AB-2002-040**
C.T. Liu *et al.*, "Stress Intensities and Crack Growth in Photoelastic Motor Grain"

Society for Experimental Mechanics 2002 Ann. Conf. **(Statement A)**
(Milwaukee, WI, 10-12 June 2002) (Deadline: 22 Mar 2002)

1. This request has been reviewed by the Foreign Disclosure Office for: a.) appropriateness of distribution statement, b.) military/national critical technology, c.) export controls or distribution restrictions, d.) appropriateness for release to a foreign nation, and e.) technical sensitivity and/or economic sensitivity.

Comments: _____

Signature _____ Date _____

2. This request has been reviewed by the Public Affairs Office for: a.) appropriateness for public release and/or b) possible higher headquarters review.

Comments: _____

Signature _____ Date _____

3. This request has been reviewed by the STINFO for: a.) changes if approved as amended, b) appropriateness of references, if applicable; and c.) format and completion of meeting clearance form if required

Comments: _____

Signature _____ Date _____

4. This request has been reviewed by PR for: a.) technical accuracy, b.) appropriateness for audience, c.) appropriateness of distribution statement, d.) technical sensitivity and economic sensitivity, e.) military/national critical technology, and f.) data rights and patentability

Comments: _____

APPROVED/APPROVED AS AMENDED/DISAPPROVED

PHILIP A. KESSEL
Technical Advisor
Space and Missile Propulsion Division

Date

STRESS INTENSITIES AND CRACK GROWTH IN PHOTOELASTIC MOTOR GRAIN MODELS

C. W. Smith, D. M. Constantinescu and C. T. Liu*

Department of Engineering Science and Mechanics
Virginia Polytechnic Institute and State University
Blacksburg, VA 24061

ABSTRACT

Preliminary studies of cracks emanating from the fin tip surface of generic photoelastic Models of Motor grain showed two preferred locations, at the confluence of an edge radius with the central radius of a fin, and on the fin axis itself. The latter cracks were planar and well behaved. The former cracks, called off-axis cracks were complex, beginning as Class II cracks and only later becoming Class I cracks. The sequel describes the stress intensity factors and crack growth surfaces measured in two basic forms of these cracks during growth.

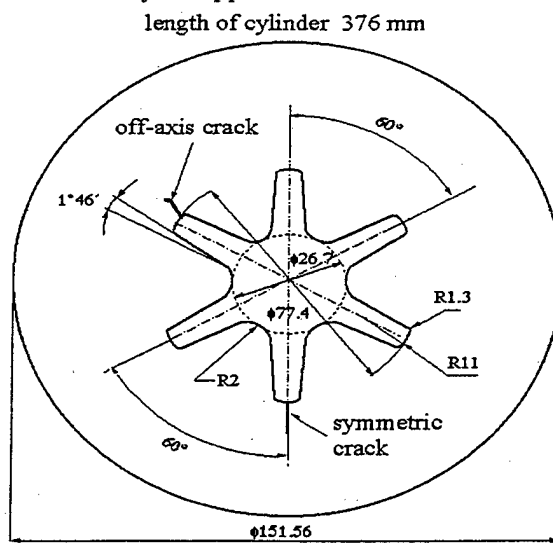
INTRODUCTION

Two dimensional thermal shrinkage tests on photoelastic models and tensile tests on single fin sections of motor grain have suggested that, for a specific fin geometry consisting of a small edge radius coalescing with a large central fin tip radius, the critical locus for stress in a homogeneous model lies at the points of confluence for the two radii on the fin surface. On the other hand, some motor grain manufacturers have reported cracks emanating from the fin tip along its own axis of symmetry as a result of defects collected there during the casting process. One aspect of the problem just beginning to be studied is how cracks grow from these two critical points. Cotterell [2] classified cracks which extended in a particular direction as Class I cracks. Those located on the axis of symmetry of a fin were such cracks which were always under Pure Mode I loading due to symmetry in both load and geometry. Other cracks, such as those emanating from the points of coalescence of the two fin tip radii (hereafter called off-axis cracks) were initially called Class II cracks, the growth direction being initially unknown due to mixed mode states along the crack border, but after

turning and growing in a new direction become Class I cracks. A series of experiments on photoelastic motor grain models under internal pressure were conducted on models containing such cracks in which the frozen stress method was used together with a two parameter algorithm in order to extract the Mode I and Mode II stress intensity factors (SIFs) at certain points along the crack borders.

THE EXPERIMENT & RESULTS

The test geometry for all models is shown in Fig. 1 together with the locus of a symmetric and an off-axis crack separated by an uncracked fin. Each model contained two starter cracks which were analyzed separately using the algorithm for converting optical data into SIF values described briefly in Appendix A.



all dimensions are in mm

Fig. 1: Model Geometry

After inserting the starter cracks by striking a shaft with a blade on the end held normal to the inner fin surface, the models were capped with RTV rubber caps which were glued with PMC-1 adhesive and were then subjected to the stress-freezing cycle under internal pressure. The cracks were grown under internal pressure above critical temperature to desired size, after which the pressure was dropped to about one third of its value and stress freezing was completed. After cooling, thin slices in the nz plane (Fig. A-1) were removed and analyzed at maximum crack depth and near the fin surface using the algorithm in Appendix A. Data and results are found in Table I where the crack projections were treated as semi-elliptic.

DISCUSSION

All of the cracks on the fin axis remained in the plane of the axis of symmetry and grew as semi-elliptic cracks. The behavior of the off-axis cracks was complicated by the presence of shear modes. Two main types of off-axis cracks were observed, neither of which were planar. The first type [Fig. 2], shown by Model #4, exhibited a semi-elliptic projected crack shape but some Mode 2 as well as Mode 1 remained. Presumably, with further extension, the crack will straighten out and eliminate Mode

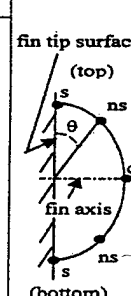
2 [3]. The second type, [Fig. 2] exhibited by Model #8, shows "river patterns" between the fin surface and maximum depth which suggests the presence of Mode 3+. Development of these patterns clearly retards the crack growth in those regions, but in the figure, growth in those regions had eliminated all shear modes so that only Mode I remained along the crack front as shown. It appeared that the river patterns were exacerbated by slight misalignments in the initial off-axis cracks.

This paper summarizes results from two tests typical of ten tests (20 cracks) on the motor grain geometry of Fig. 1. On the basis of these studies, which covered cracks of projected a/c values of 0.5 to 0.9 and a/t values from 0.2 to 0.6, it appears that both SIF values and crack geometry during growth are quite variable due to shear modes during the class II stage for the off-axis cracks. On the other hand the "symmetric" cracks on the fin axis are quite predictable in their behavior (as are the off-axis cracks after eliminating the shear modes).

During the test program, it was noticed that the cracks along the fin axis tended to grow much more readily than the off-axis cracks, always in the plane of the fin axis. The off-axis cracks, once the shear modes were eliminated by turning, tended to follow the direction of the fin axis towards the outer boundary of the motor grain.

Table I

Loads ¹	Crack Description ² (dimensions in mm)	³ $F_i = K_i \sqrt{Q} / p_{sf} \sqrt{\pi a}$ $i = 1, 2$		
		depth (d)	surface (s)	
			top	bottom
$P = 88.97 \text{ N}$ $P_{max} = 0.049 \text{ MPa}$ $p_{sf} = 0.035 \text{ MPa}$	Model 4 Off-axis inclined $a = 8.71$ $\Delta a = 2.18$ $c = 11.15$ $\Delta c = 3.02$ $a/c = 0.78$ $a/t = 0.23$	$F_1 = 1.90$ $F_2 = 0.48$	ns 20° 2.62*	ns 20° 2.55*
	Model 8 Off-axis inclined $a = 12.50$ $\Delta a = 3.4$ $c = 21.1$ $\Delta c = 10.4$ $a/c = 0.59$ $a/t = 0.34$		ns 30° 2.12*	ns 30° 2.13*
		* F_i values		



Notations:

1. P = axial compressive load
 P_{max} = maximum internal pressure to grow crack
 p_{sf} = stress freezing pressure
2. a = crack depth; Δa = crack length growth
 c = half length of crack in fin tip surface; Δc = half crack growth in fin tip surface
3. \sqrt{Q} = approximation of elliptic integral of second kind

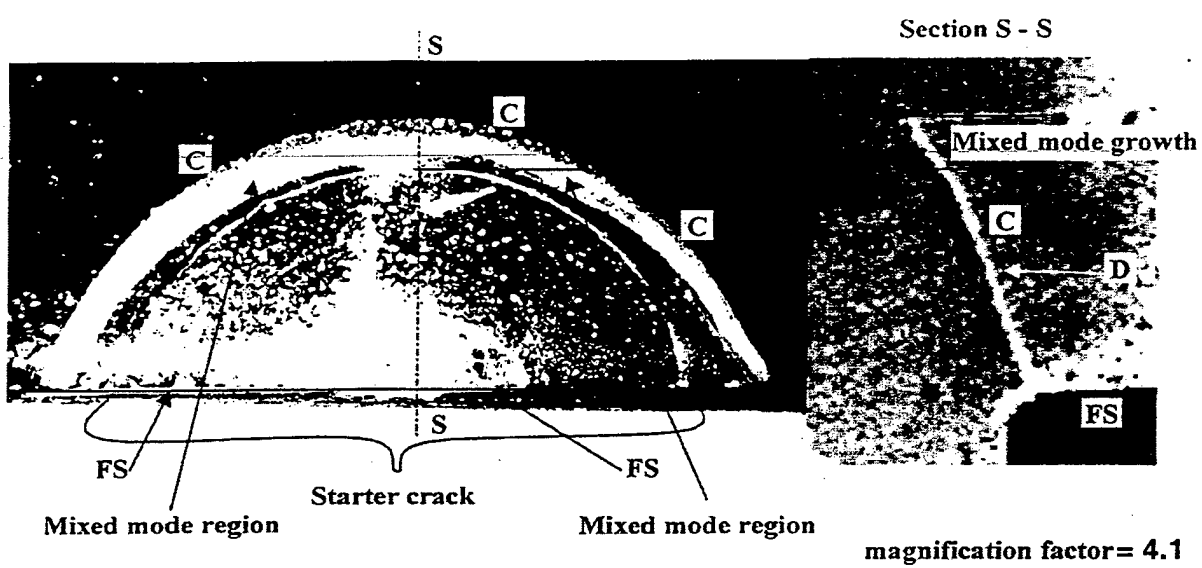
$$Q = 1 + 1.464 \left(\frac{a}{c} \right)^{1.65} \quad \frac{a}{c} \leq 1$$

$$Q = 1 + 1.464 \left(\frac{c}{a} \right)^{1.65} \quad \frac{a}{c} > 1$$

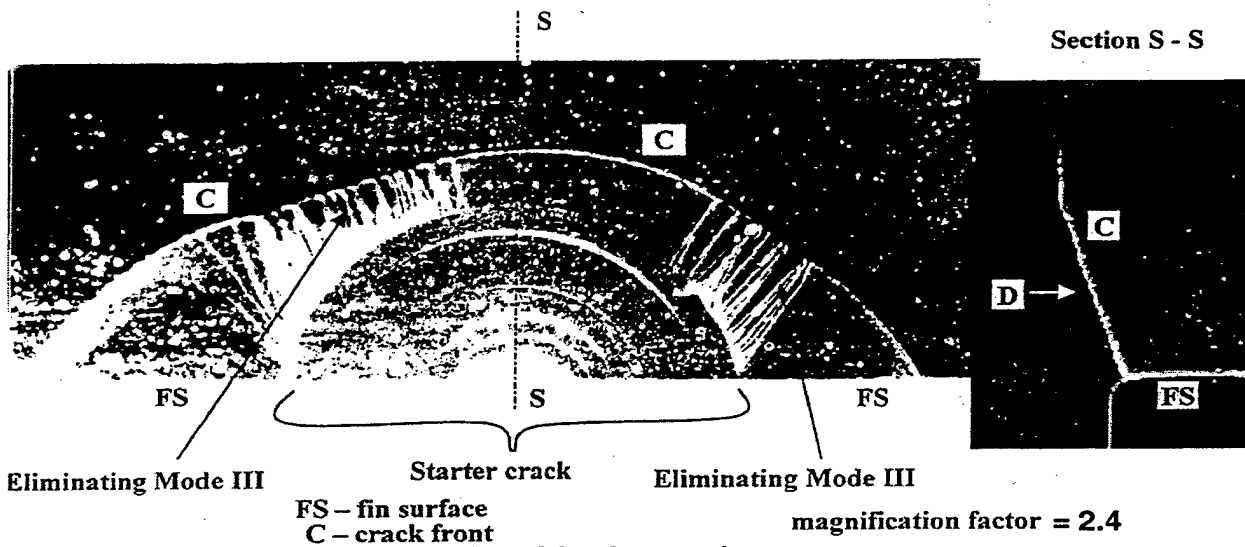
All flaws were characterized as semi-elliptic flaws of depth a and length $2c$. However, off-axis cracks were neither perfectly semi-elliptic nor planar.

4. ns = near surface slices were used in place of surface slices to avoid a possible surface fringe
5. Slices at $\theta = 60^\circ$ revealed a shear mode in Model 4 but not in Model 8.

⁺ Since the river patterns involve a separation of the fracture surface along them, no calculations can be made for Mode 3.



Model 4 Off-Axis Inclined Crack Showing Starter Crack and Final Crack Front



Model 8 Off-Axis Inclined Crack Showing Starter Crack and Final Mode I Crack Front

Fig. 2: Projected Crack Profiles and Path of Center-point

ACKNOWLEDGEMENT

The authors gratefully acknowledge the support of the above studies under P. O. # RPO10230 with ERC Inc. through AFRL.

REFERENCES

1. Smith, C. W., Constantinescu, D. M. and Liu, C. T., "Stress Intensity Factors and Paths for Cracks in Photoelastic Motor Grain Models Under Internal Pressure," *Recent Advances in Solids and Structures ASME-PVP Symposium Proceedings IMECE 2001 PVP-25200* New York, NY, November 2001.
2. Cotterell, B., "On Brittle Fracture Paths," *International Journal of Fracture Mechanics*, Vol. 1, pp. 96-103, 1965.
3. Smith, C. W., Constantinescu, D. M. and Liu, C. T., "Observations on Crack Turning by Optical Methods," *Advances in Computational and Engineering Sciences*, Chapter 9, Paper No. 8, Aug. 2001.
4. Smith, C. W. and Kobayashi, A. S., "Experimental Fracture Mechanics," Chapter 20 of *Handbook on Experimental Mechanics*, 2nd Revised Ed. pp. 905-968, 1993.

APPENDIX A

(Mode I Algorithm)

Beginning with the Giffith-Irwin Equations, we may write, for Mode I, for the homogeneous case

$$\sigma_{ij} = \frac{K_1}{(2\pi r)^{\frac{1}{2}}} f_{ij}(\theta) + \sigma_{ij}^o \quad (i, j = n, z) \quad (1)$$

where: σ_{ij} are components of stress, K_1 is SIF, r, θ are measured from crack tip (Fig. A-1), σ_{ij}^o are non-singular stress components.

Then, along $\theta = \pi/2$, after truncating σ_{ij}

$$(\tau_{nz})_{max} = \frac{K_1}{(8\pi r)^{\frac{1}{2}}} + \tau^o = \frac{K_{AP}}{(8\pi r)^{\frac{1}{2}}} \quad (2)$$

where $\tau^o = f(\sigma_{ij}^o)$ and is constant over the data range, K_{AP} = apparent SIF, τ_{nz} = maximum shear stress in nz plane

$$\therefore \frac{K_{AP}}{\bar{\sigma}(\pi a)^{\frac{1}{2}}} = \frac{K_1}{\bar{\sigma}(\pi a)^{\frac{1}{2}}} + \frac{\sqrt{8}\tau^o}{\bar{\sigma}} \left(\frac{r}{a} \right)^{\frac{1}{2}} \quad (3)$$

where (Fig. A-1) a = crack length, and $\bar{\sigma}$ = remote normal stress i.e.

$$\frac{K_{AP}}{\bar{\sigma}(\pi a)^{\frac{1}{2}}} \text{ vs. } \sqrt{\frac{r}{a}} \text{ is linear.}$$

Since from the Stress-Optic Law $(\tau_{nz})_{max} = nf/2t$ where, n = stress fringe order, f = material fringe value, t = specimen (or slice) thickness, then from Eq. 2,

$$K_{AP} = (8\pi r)^{\frac{1}{2}} (\tau_{nz})_{max} = (8\pi r)^{\frac{1}{2}} nf/2t$$

A typical plot of normalized K_{AP} vs. $\sqrt{r/a}$ for a homogeneous specimen is shown in Fig. A-2. For mixed mode analysis, see [4].

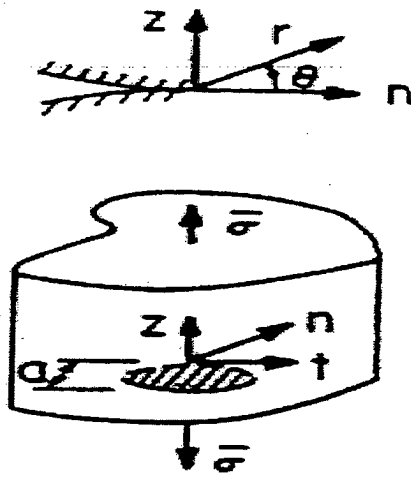


Fig. A-1: Mode I Near Tip Notation

Model 8, off-axis inclined,
 $a/t = 0.59$, $a/t = 0.34$, depth (d)

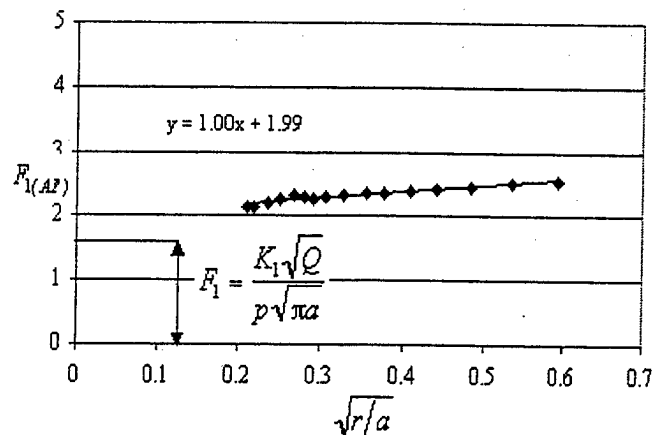


Fig. A-2 Determination of F_1 from Test Data